

# $^{31}\text{P}$ NMR Studies Demonstrating the Assembly of *catena*-Phosphorus Frameworks from Chlorophosphinochlorophosphonium Cations

Yuen-ying Carpenter,<sup>†</sup> Neil Burford,<sup>\*,†</sup> Michael, D. Lumsden,<sup>‡</sup> and Robert McDonald<sup>§</sup>

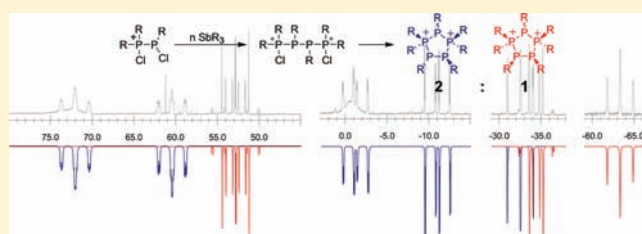
<sup>†</sup>Department of Chemistry, Dalhousie University, Halifax, NS, B3H 4J3, Canada

<sup>‡</sup>Nuclear Magnetic Resonance Research Resource (NMR-3), Dalhousie University, Halifax, NS, B3H 4J3, Canada

<sup>§</sup>X-ray Crystallography Laboratory, Department of Chemistry, University of Alberta, Edmonton, Alberta T6G 2G2, Canada

**S** Supporting Information

**ABSTRACT:** New examples of chlorophosphinochlorophosphonium (4) and chlorophosphinodichlorophosphonium (5) cations have been prepared and spectroscopically characterized. These bifunctional phosphinophosphonium cations offer a new approach to the development of phosphinophosphonium frameworks using reductive coupling reactions and have been exploited as synthons to assemble larger *catena*-phosphorus cations. The reactions of 4 and 5 with stibine reducing agents have been studied using  $^{31}\text{P}$  NMR spectroscopy and have been shown to produce a variety of new and known frameworks in a facile manner, depending on the reducing agent selection and the stoichiometry of the reaction. New derivatives of frameworks containing three, four, and five phosphorus atoms have been identified by  $^{31}\text{P}$  NMR spectroscopy. Crystals of the  $[\text{GaCl}_4]^-$  salt of the five-membered dication **11** (<sup>i</sup>Pr) have been isolated from the reaction of  $[\text{4}^{\text{iPr}}][\text{GaCl}_4]^-$  with  $\text{SbBu}_3$ , and the solid state structural features and solution state dynamics are comprehensively described in the context of  $^{31}\text{P}\{^1\text{H}\}$  NMR spectroscopic observations.

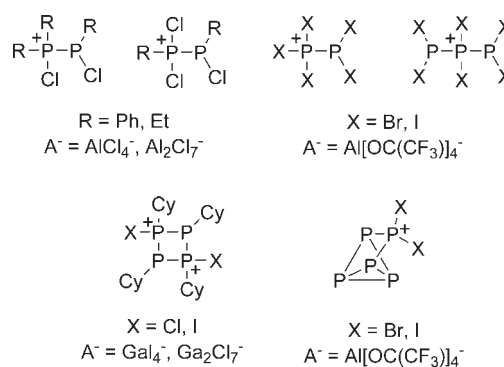


## INTRODUCTION

A variety of synthetic approaches to *catena*-phosphinophosphonium cations have been developed that give access to a series of frameworks demonstrating the potential for systematic extension and diversification of *catena*-phosphorus chemistry.<sup>1</sup> The reactions are often high yielding due to the presence of the molecular positive charge, which presumably provides for a distinct low energy reaction pathway. The prototypical phosphinophosphonium (1) framework is readily derivatized with chlorine substituents at either the phosphine (2)<sup>2,3</sup> or phosphonium center (3).<sup>4,5</sup> In this context, the well-known reduction of chlorophosphines to give diphosphines and cyclopolyphosphines<sup>6</sup> can be applied to chlorophosphinophosphonium cations 2 to give 2,3-diphosphino-1,4-diphosphonium cations 7,<sup>2,3</sup> as illustrated in eq 1.

The application of reductive coupling to generate new polyphosphorus cations requires small halogenated cationic building blocks, few examples of which have been reported (Chart 1).<sup>7–14</sup> To exploit this methodology, we have prepared a series of new derivatives of chlorophosphinochlorophosphonium (4) and chlorophosphinodichlorophosphonium cations (5) as tetrachlorogallate salts and have used  $^{31}\text{P}$  NMR spectroscopy to study reactions with  $\text{SbPh}_3$  or  $\text{SbBu}_3$ , which effect reductive coupling and the assembly of larger *catena*-phosphorus frameworks (Chart 2). Here, we report the spectroscopic identification of a series of *catena*-phosphinophosphonium frameworks as well as the isolation and structural characterization of a *cyclo*-phosphinodiphosphonium salt.

**Chart 1. Known Poly-Halide Functionalized *catena*-Phosphorus Cations**



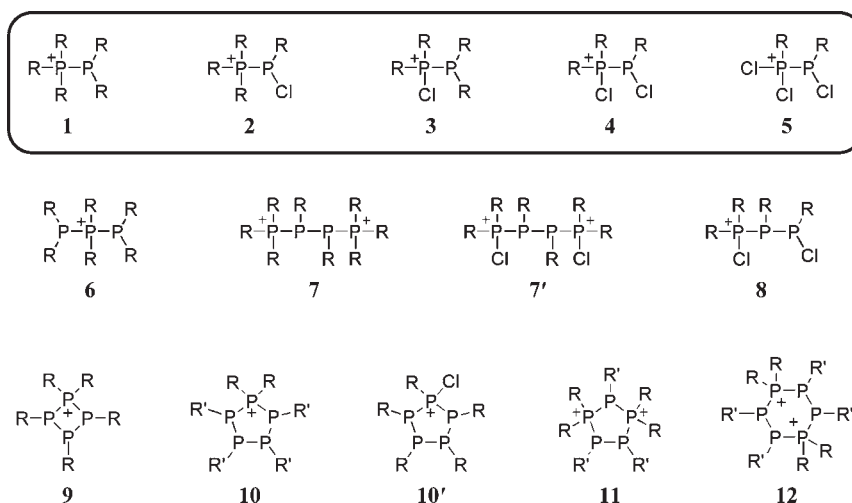
## RESULTS AND DISCUSSION

Reaction mixtures of a chlorophosphine ( $\text{R}_2\text{P}(\text{Cl})$ ) with a halide abstracting agent ( $\text{Abs} = \text{AlCl}_3, \text{GaCl}_3$  for any  $\text{R} = \text{aryl, alkyl}$ ;  $\text{Me}_3\text{SiOTf}$  also for  $\text{R} = \text{Me}$ ) quantitatively form phosphinochlorophosphonium cations 3, as shown in eq 2. The process can be envisaged to involve the formation of a Lewis acidic phosphonium cation  $[\text{PR}_2]^+$  and subsequent coordination of the chlorophosphine ligand. This procedure has here been extended to the

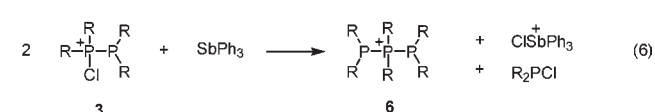
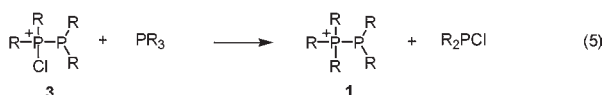
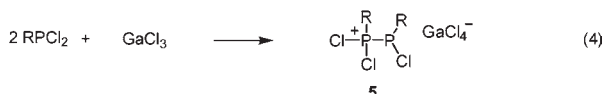
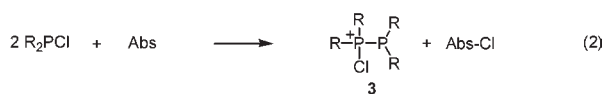
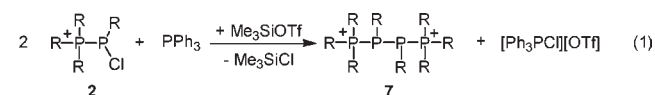
**Received:** October 25, 2010

**Published:** March 25, 2011

Chart 2. Representative Phosphinophosphonium Cation Frameworks



reaction of dichlorophosphines (eqs 3 and 4), where  $^{31}\text{P}\{^1\text{H}\}$  NMR spectra of reaction mixtures show the quantitative formation of  $4[\text{GaCl}_4]$  and  $5[\text{GaCl}_4]$ , respectively. Chemical shifts and coupling constants for all derivatives are summarized in Table 1.  $^{31}\text{P}\{^1\text{H}\}$  NMR spectra for derivatives of **4** are sufficiently resolved at room temperature to distinguish  $^1J_{\text{PP}}$ , but spectra for derivatives of **5** contain broad peaks, perhaps indicating dynamic dissociation of the coordinate P–P bond due to the comparatively weak donation from the dichlorophosphine. Attempts to prepare dichlorophosphinophosphonium cations using these methods showed no evidence of reaction or yielded salts of triphosphenium cations  $[\text{R}_3\text{P}-\text{P}-\text{PR}_3]^+$ .<sup>15</sup>



In contrast to reactions of 1-chloro-1-phosphino-2-phosphonium cations (**2**) with  $\text{PPh}_3$  according to eq 1,<sup>2,3</sup> the isomeric 1-phosphino-2-chloro-2-phosphonium cations (**3**) react with

$\text{PPh}_3$  or trialkylphosphines via ligand exchange to produce the prototypical phosphinophosphonium cations (**1**), illustrated in eq 5.<sup>4,5</sup> Interestingly, reactions of derivatives of  $3[\text{GaCl}_4]$  with the less nucleophilic reductant  $\text{SbPh}_3$  yield tetrachlorogallate salts of 1,3-diphosphino-2-phosphonium cations (**6**), as illustrated in eq 6. We envisage this reaction to proceed via formal chloronium abstraction from **3** by  $\text{SbPh}_3$  to give a diphosphine and a chlorostibonium cation. The diphosphine competes with  $\text{R}_2\text{P}^+\text{Cl}$  as a ligand, effecting ligand exchange on **3** to give **6**, as proposed in Scheme 1.  $^{31}\text{P}\{^1\text{H}\}$  NMR spectra of reaction mixtures indicate that **3** is not completely consumed in the reaction with  $\text{SbPh}_3$ , whereas reduction with  $\text{SbBu}_3$  effects quantitative formation of the extended framework **6**. Reaction with 1 equivalent of  $\text{SbBu}_3$  effects not only reduction of **3** to **6**, but also reduction of the *in situ* generated  $\text{R}_2\text{P}^+\text{Cl}$  to the diphosphine, resulting in exchange-broadened  $^{31}\text{P}$  NMR spectra. The addition of  $\text{GaCl}_3$  to the reaction mixture with either reductant instead regenerates **3** from the eliminated chlorophosphine, as in eq 2.

Reaction mixtures of chlorophosphinochlorophosphonium cations (**4**) with either  $\text{SbPh}_3$  or  $\text{SbBu}_3$  show a number of products in the  $^{31}\text{P}\{^1\text{H}\}$  NMR spectra depending on the reaction stoichiometry. The addition of 1 equivalent of  $\text{SbPh}_3$  to  $[\mathbf{4}(\text{Ph})][\text{GaCl}_4]$  in  $\text{CH}_2\text{Cl}_2$  results in a mixture of  $[\mathbf{10}(\text{Ph})][\text{GaCl}_4]$ ,<sup>17</sup>  $[\mathbf{12}(\text{Ph})][\text{GaCl}_4]_2$ ,<sup>18</sup> and  $[\mathbf{3}(\text{Ph})][\text{GaCl}_4]$  as the major products after 12 h (summarized in Table 2a). The addition of 2 equivalents of  $\text{SbPh}_3$  to  $[\mathbf{4}(\text{Ph})][\text{GaCl}_4]$  gives a similar product distribution, with  $[\mathbf{6}(\text{Ph})][\text{GaCl}_4]$  as a minor product. In contrast, the addition of 2 equivalents of the stronger reductant  $\text{SbBu}_3$  to  $[\mathbf{4}(\text{Ph})][\text{GaCl}_4]$  gives the more reduced (less charged) species,  $[\mathbf{10}(\text{Ph})][\text{GaCl}_4]$  and  $\text{Ph}_2\text{P}-\text{PPh}_2$ . The addition of 1.5 equivalents of  $\text{SbBu}_3$  to  $[\mathbf{4}(\text{Ph})][\text{GaCl}_4]$  yields  $[\mathbf{10}(\text{Ph})][\text{GaCl}_4]$  with  $\text{Ph}_2\text{P}-\text{PPh}_2$  and  $[\mathbf{6}(\text{Ph})][\text{GaCl}_4]$ . The addition of less than 1 equivalent of either reducing agent results in incomplete consumption of **4**.

The addition of 2 equivalents of  $\text{SbPh}_3$  and 1 equivalent of  $\text{GaCl}_3$  to  $\mathbf{4}(\text{Ph})$  results in nearly quantitative conversion to the dication  $\mathbf{12}(\text{Ph})$ . The previously observed decomposition<sup>18</sup> of  $[\mathbf{12}(\text{Ph})][\text{GaCl}_4]_2$  to the five-membered monocation  $[\mathbf{10}(\text{Ph})][\text{GaCl}_4]$  ( $t_{1/2} = 24$  h) in solution is negligible in this mixture. This preference for the more charged species is effected by the

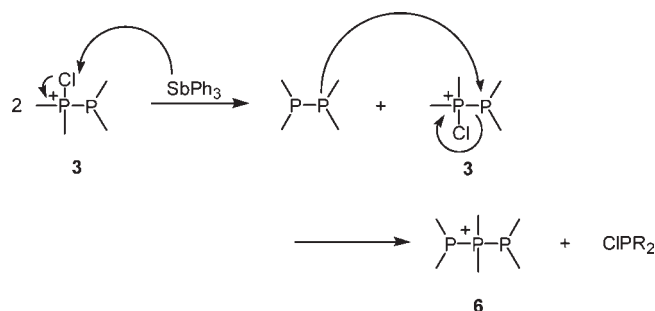
Table 1.  $^{31}\text{P}\{^1\text{H}\}$  NMR Parameters for Selected Phosphinophosphonium Gallate Salts<sup>a</sup>

cation	donor	acceptor	spin system	$\delta_{\text{BorX}}$ [ppm] (phosphonium)	$\delta_{\text{A}}$ [ppm] (phosphine)	$^1J_{\text{PP}}$ [Hz] (T) <sup>b</sup>
3(Ph) <sup>16</sup>	Ph <sub>2</sub> (Cl)P	PPh <sub>2</sub>	AX	73	0	−393
4(Ph) <sup>c</sup>		PPh(Cl)	AB	72	57	−395
5(Ph) <sup>c</sup>	Ph(Cl) <sub>2</sub> P	PPh(Cl)		131	81–85	broad (213 K)
3(Me) <sup>16</sup>	Me <sub>2</sub> (Cl)P	PMe <sub>2</sub>	AX	99	−33	−340
4(Me)		PMe(Cl)	AB	93	74	−365
5(Me)		PMe(Cl)	AX	154	97	−400 (213 K)
3(Et) <sup>d</sup>	Et <sub>2</sub> (Cl)P	PEt <sub>2</sub>	AX	109	−19	−378
4(Et) <sup>c</sup>		PEt(Cl)	AB	107	79	−391
5(Et) <sup>c</sup>	Et(Cl) <sub>2</sub> P	PEt(Cl)	AX	137	92	−446 (193 K)
4( <sup>t</sup> Pr)	<sup>t</sup> Pr <sub>2</sub> (Cl)P	P <sup>t</sup> Pr(Cl)	AB	110	93	−431
4(Cy)	Cy <sub>2</sub> (Cl)P	PCy(Cl)	AB	101	88	−437
4(Ph <sub>2</sub> /Me)	Ph <sub>2</sub> (Cl)P	PMe(Cl)	AB	76	72	−378

<sup>a</sup> Substituents are indicated in parentheses in cation labels 3(R), 4(R), and 5(R). Data are reported for spectra obtained in CH<sub>2</sub>Cl<sub>2</sub> at 101.3 MHz.

<sup>b</sup> Spectra recorded at 298 K unless otherwise indicated. <sup>c</sup>  $^{31}\text{P}$  NMR spectra are consistent with previously reported [Al<sub>x</sub>Cl<sub>y</sub>]<sup>−</sup> derivatives. <sup>d</sup> Correction to previously reported  $^{31}\text{P}$  NMR data for this compound.<sup>16</sup>

### Scheme 1. Proposed Mechanism for a Reductive Coupling Chain Extension of 3, As Observed in eq 6



comparatively weak reducing agent (SbPh<sub>3</sub> vs SbBu<sub>3</sub>) as well as the *in situ* formation of the [Ga<sub>2</sub>Cl<sub>7</sub>]<sup>−</sup> anion from [GaCl<sub>4</sub>]<sup>−</sup>. The addition of excess GaCl<sub>3</sub> suppresses the equilibrium dissociation of [GaCl<sub>4</sub>]<sup>−</sup> to yield chloride, which is proposed to undergo nucleophilic attack on the dication 12.

The reductive coupling of [4(Me)][GaCl<sub>4</sub>] (summarized in Table 2b) demonstrates a thermodynamic preference for the five-membered dicationic ring [11(Me)][GaCl<sub>4</sub>]<sub>2</sub><sup>19</sup> over the six-membered alternative. Likewise, the reaction of [4(Et)][GaCl<sub>4</sub>] with 1 equivalent of SbBu<sub>3</sub> yields a mixture of [3(Et)][GaCl<sub>4</sub>] with 10(Et) and [11(Et)][GaCl<sub>4</sub>]<sub>2</sub> (summarized in Table 2c). In contrast, the  $^{31}\text{P}$  NMR spectrum of the reaction mixture of SbPh<sub>3</sub> with GaCl<sub>3</sub> and [4(Et)][GaCl<sub>4</sub>] indicates nearly quantitative formation of [Et<sub>2</sub>(Cl)P–PEt–PEt–P(Cl)Et<sub>2</sub>][GaCl<sub>4</sub>]<sub>2</sub>, [7'(Et)][GaCl<sub>4</sub>]<sub>2</sub>, identified by the characteristic AA'XX' spin system shown in Figure 1. Attempted crystallization of [7'(Et)][GaCl<sub>4</sub>]<sub>2</sub> by slow evaporation over a period of weeks resulted in the precipitation of a yellow solid identified as [11(Et)][GaCl<sub>4</sub>]<sub>2</sub> ( $^{31}\text{P}\{^1\text{H}\}$  NMR parameters: Table 4), suggesting that 7' is a kinetically stabilized intermediate en route to 11 (Scheme 2). In the analogous reduction reaction of [Ph<sub>2</sub>(Cl)P–PMeCl][GaCl<sub>4</sub>], 4(Ph<sub>2</sub>/Me), the kinetic product 7'(Ph<sub>2</sub>/Me) was observed in the reaction solution according to  $^{31}\text{P}\{^1\text{H}\}$  NMR spectroscopy for less than 22 h prior to its complete conversion to the thermodynamically favored

dicationic ring 11(Ph<sub>2</sub>/Me). While all other known derivatives of 11 adopt a *trans* orientation of substituents at the adjacent phosphine sites, 11(Ph<sub>2</sub>/Me) was consistently produced as a 2:1 mixture of the *trans* and *cis* isomers (Figure 2). The higher (C<sub>s</sub>) symmetry of the *cis* isomer readily distinguishes it as an ABB'XX' spin system in  $^{31}\text{P}\{^1\text{H}\}$  NMR spectra. The magnitude of the one-bond coupling constant between the phosphine sites (P4/P5) was observed to be substantially larger in the *cis* isomer ( $^1J_{\text{PP}(\text{cis})} = -323$  Hz;  $^1J_{\text{PP}(\text{trans})} = -260$  Hz). This is in agreement with previous experimental<sup>20–22</sup> and theoretical<sup>23,24</sup> studies indicating the substantial stereochemical dependence of  $^{31}\text{P}$ – $^{31}\text{P}$  coupling constants—specifically, that coupled phosphorus nuclei with *cis*-oriented lone pairs exhibit one-bond coupling constants that are substantially greater than their *trans*-oriented analogues, i.e.,  $|^1J_{\text{PP}(\text{cis})}| > |^1J_{\text{PP}(\text{trans})}|$ .<sup>6,22,24</sup> In addition, the  $^{31}\text{P}$  NMR chemical shifts of all three phosphine sites in the *cis* isomer are considerably upfield shifted relative to the *trans* isomer ( $\Delta\delta = 25$ – $35$  Hz). Although rare among *cis*–*trans* isomers of neutral cyclopolyphosphines, such a large magnitude difference in chemical shift has been previously observed in the case of *cyclo*-(<sup>t</sup>BuP)<sub>2</sub>P<sup>t</sup>Pr.<sup>6</sup> [11(Ph<sub>2</sub>/Me)][GaCl<sub>4</sub>]<sub>2</sub> represents, however, the first observation of adjacent *cis* substituents in a cationic catena-phosphorus ring system.

Crystals of [11(<sup>t</sup>Pr)][GaCl<sub>4</sub>]<sub>2</sub> have been isolated from the reaction of [4(<sup>t</sup>Pr)][GaCl<sub>4</sub>] with SbBu<sub>3</sub>. Views of the cation are shown in Figure 3. Using the PLATON software package,<sup>25</sup> the solid state structure of [11(<sup>t</sup>Pr)][GaCl<sub>4</sub>]<sub>2</sub> was determined to approximate an <sup>4</sup>E envelope conformation with a Cremer–Pople<sup>26</sup> phase angle ( $\varphi$ ) of 286.80(5)<sup>o</sup> and puckering amplitude ( $Q$ ) of 0.9040(7) Å. Bond lengths and angles within the ring are generally comparable to those observed for the two previously reported<sup>19</sup> cyclo-triphosphino-1,3-diphosphonium cations (Table 3), although the angle about one phosphonium center (P3) is significantly smaller in 11(<sup>t</sup>Pr), presumably as a result of substituent steric strain. The closest cation–anion contact is a Cl–H interaction at 2.68 Å ( $\Sigma r_{\text{vdw}} = 2.84$  Å) between a tetrachlorogallate anion and a methyl proton of one isopropyl group in the adjacent asymmetric unit.

Simulation of the AGHMX spin system apparent in  $^{31}\text{P}$ – $\{^1\text{H}\}$  NMR spectra of solutions of 11(<sup>t</sup>Pr) at 188 K (Figure 4,

Table 2. Products Observed for Reductive Coupling Reactions<sup>a</sup> of  $[\text{R}_2(\text{Cl})\text{P}-\text{PR}'\text{Cl}][\text{GaCl}_4]$  Including (a) 4(Ph), (b) 4(Me), and (c) 4(Et)<sup>b</sup>

High	> 70	
Moderate	41-70	
Low	10-40	
Negligible	< 10	

Products \ Reagents					
	12(Ph)	10(Ph)	3(Ph)	6(Ph)	4(Ph)
2 SbPh <sub>3</sub> 1 GaCl <sub>3</sub>					
1-2 SbPh <sub>3</sub> or 1 SbBu <sub>3</sub> <sup>b</sup>					
1.5 SbBu <sub>3</sub>					
2 SbBu <sub>3</sub>					

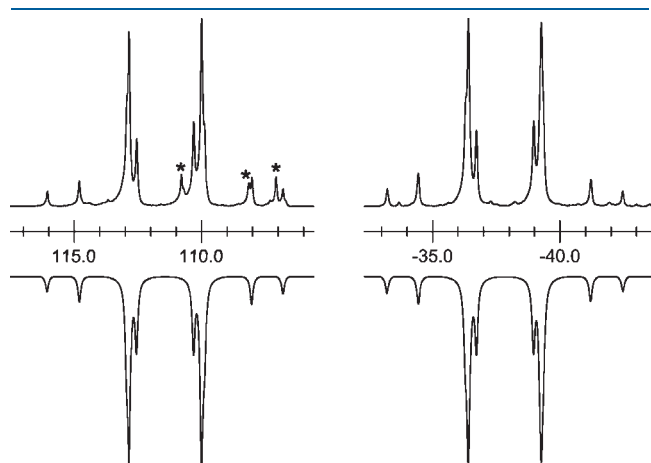
Products \ Reagents					MePCl <sub>2</sub>
	11(Me) <sup>c</sup>	10(Me)	3(Me)	6(Me)	
1 SbPh <sub>3</sub>	present				
1 SbBu <sub>3</sub>	present				
1 SbBu <sub>3</sub> (solvent: MeCN)					
2 SbBu <sub>3</sub> (solvent: MeCN)					

Products \ Reagents						
	11(Et)	10(Et) <sup>d</sup>	9(Et) <sup>e</sup>	7'(Et)	3(Et)	6(Et)
2 SbPh <sub>3</sub> 1 GaCl <sub>3</sub>						
1 SbBu <sub>3</sub>						
1 SbBu <sub>3</sub> 1 GaCl <sub>3</sub> <sup>f</sup>						
2 SbBu <sub>3</sub>						

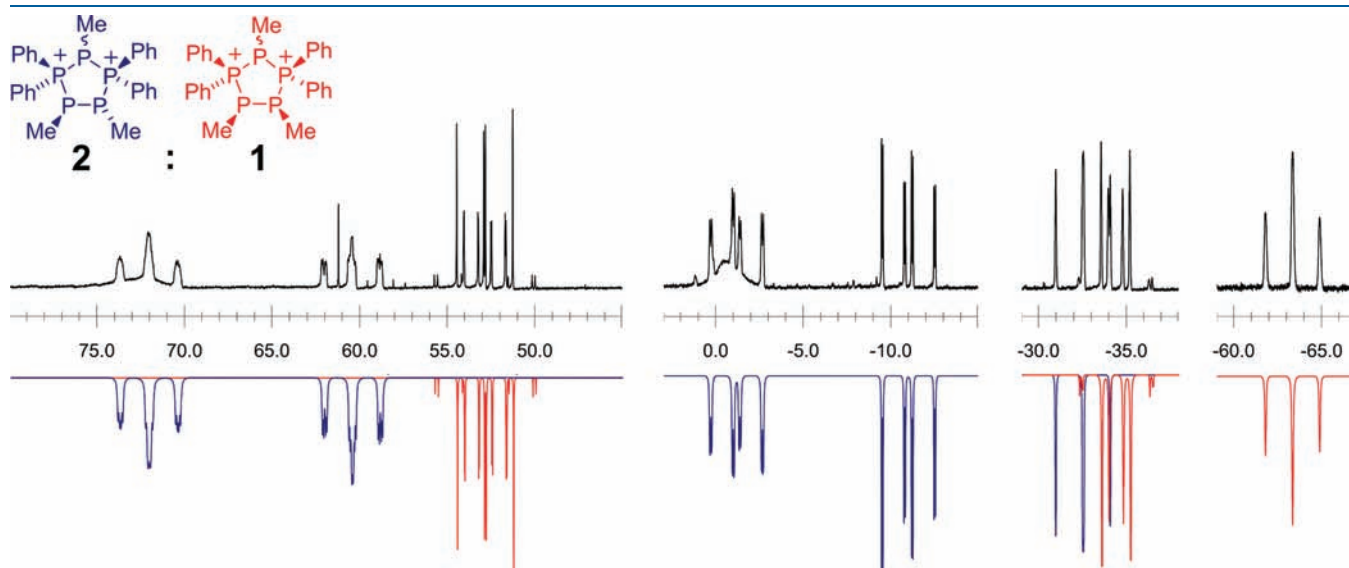
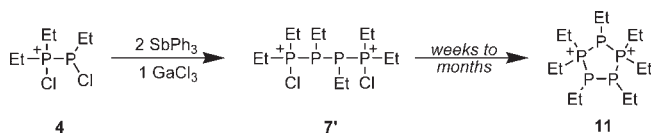
<sup>a</sup>All reactions conducted in CH<sub>2</sub>Cl<sub>2</sub> unless otherwise noted. <sup>b</sup>Relative conversion (based on the area of the <sup>31</sup>P{<sup>1</sup>H} NMR signals) to each of the products vs. the most predominant species (assigned as 100) is indicated by shading according to the ranges shown in the key at the top. <sup>c</sup>Also contains a moderate amount of PhPCl<sub>2</sub>. <sup>d</sup>[11(Me)][GaCl<sub>4</sub>]<sub>2</sub> was isolated as a precipitate from CH<sub>2</sub>Cl<sub>2</sub> reactions and redissolved in MeCN to confirm its identity by <sup>31</sup>P{<sup>1</sup>H} NMR spectroscopy. Relative abundance could not be assessed by NMR, so shading indicates only the presence or absence of this product in these reactions. <sup>e</sup><sup>31</sup>P{<sup>1</sup>H} NMR parameters could not be simulated due to overlap with other products (approximate chemical shifts: δ = 91 ± 1, 12 ± 3, and -3 ± 4 ppm). <sup>f</sup><sup>31</sup>P{<sup>1</sup>H} NMR parameters, A<sub>2</sub>BX system: δ<sub>A</sub> = -62.3, δ<sub>A</sub> = -54.4, δ<sub>X</sub> = 12.5 ppm; <sup>1</sup>J<sub>AB</sub> = -225, <sup>1</sup>J<sub>BX</sub> = -112, <sup>2</sup>J<sub>AX</sub> = 21. <sup>g</sup>Also contains Et<sub>2</sub>P-PEt<sub>2</sub> (δ<sub>31P</sub> = -25 ppm, broad singlet) as a major product.

Table 4) yields chemical shift and coupling constant parameters that are comparable to those of known derivatives<sup>19</sup> of **11**. However,  $^1J_{PP}$  between the backbone phosphorus atoms P4–P5 was observed to be significantly smaller in magnitude (–149 Hz) for **11**(<sup>i</sup>Pr) relative to other derivatives of **11** with *trans*-oriented substituents (–260 to –315 Hz). Although all derivatives in Table 4 are *trans*-



**Figure 1.** Experimental (upright) and simulated (inverted) expansions of the  $^{31}\text{P}\{^1\text{H}\}$  NMR spectra of  $[7'(\text{Et})][\text{GaCl}_4]_2$  in the reaction mixture of  $[4(\text{Et})][\text{GaCl}_4]$  with  $2\text{SbPh}_3$  and  $\text{GaCl}_3$ . Minor impurities in the reaction mixture are marked with asterisks.

#### Scheme 2. Conversion of $[7'(\text{Et})][\text{GaCl}_4]_2$ to $[11(\text{Et})][\text{GaCl}_4]_2$



**Figure 2.** Experimental (upright) and simulated (inverted) expansions of the  $^{31}\text{P}\{^1\text{H}\}$  NMR spectrum at 202.6 MHz of the 2:1 mixture of *trans* (blue) and *cis* (red) isomers of **11**( $\text{Ph}_2/\text{Me}$ ), with characteristic AGHMX and ABB'XX' spin systems, respectively. Broad peaks at 0.5 and 72 ppm (not simulated) correspond to the phosphinophosphonium cation **3**(Ph).

substituted, the magnitude of  $^nJ_{PP}$  is expected to depend more specifically on the relative lone pair orientation ( $\varphi_{LP}$ ) of the phosphorus atoms in question.<sup>24</sup>  $\varphi_{LP}$  may be formally defined by the dihedral angle between the bisectors of the R–P–R angle at each phosphorus atom and is therefore inversely proportional to the dihedral angle between the substituents. Among the three crystallographically characterized derivatives of **11**, there is substantial variation in the C–P4–P5–C dihedral angle between the *trans*-oriented substituents in the solid state (Table 3). The observed C–P4–P5–C dihedral angle in **11**(<sup>i</sup>Pr) ( $93^\circ$ ) implies a large  $\varphi_{LP}$  angle and a correspondingly small magnitude  $^1J_{P4P5}$  relative to **11''** (C–P4–P5–C  $143^\circ$ ).

$^{31}\text{P}\{^1\text{H}\}$  NMR analysis of EtCN solutions of crystalline  $[\mathbf{11}(\text{Pr})][\text{GaCl}_4]_2$  at a variety of temperatures revealed substantial peak broadening near room temperature (Figure 5), indicative of dynamic behavior in solution. It is particularly noteworthy that the resonance attributed to P2 (–44 ppm [291 K] to –53 ppm [188 K]) appeared sharp, with a line shape that was relatively invariant as a function of the temperature, implying that the solution exchange process(es) occur remotely from the position of this atom. Further, low temperature  $^{31}\text{P}$  NMR data for **11**(<sup>i</sup>Pr) suggests a molecule with  $C_1$  symmetry, whereas, at high temperatures, the observed AMM'XX' spin system suggests effectively time-averaged  $C_2$  or  $C_s$  symmetry. A survey of existing five-membered ring systems (I,<sup>22,27,28</sup> II,<sup>29</sup> III,<sup>30</sup> IV,<sup>31</sup> and **10**<sup>17</sup>) with a predominantly *catena*-phosphorus frame indicate a preference for low symmetry ( $C_1$ ) solid state structures, with varied symmetry in solution ( $C_1$  symmetry (ABCDX) for two derivatives of **10**,<sup>17</sup>  $[(\text{PhP})_4\text{PPhMe}][\text{OTf}]$  and  $[(\text{PhP})_4\text{PPh}^t\text{Bu}][\text{GaCl}_4]$ , and higher symmetry for I<sup>22</sup> (AA'BB'C), II<sup>29</sup> (ABB'CC'), III<sup>32</sup> (AA'BB'), and IV<sup>31</sup> (ABCD at –100 °C; AA'BB' at 60 °C) and other derivatives of **10** (AA'BB'X),<sup>17</sup>  $[\mathbf{10}(\text{Me})][\text{OTf}]$ ,  $[\mathbf{10}(\text{Me}_2/\text{Cy})][\text{OTf}]$ ,  $[\mathbf{10}(\text{Ph})][\text{OTf}]$ , and  $[\mathbf{10}(\text{Me}_2/\text{Ph})][\text{OTf}]$ ). These observations have been previously rationalized by invoking inversion at phosphorus, static solution  $C_2$  or  $C_s$  conformations, or pseudorotation (ring-puckering) processes. To understand the fluxional process occurring in

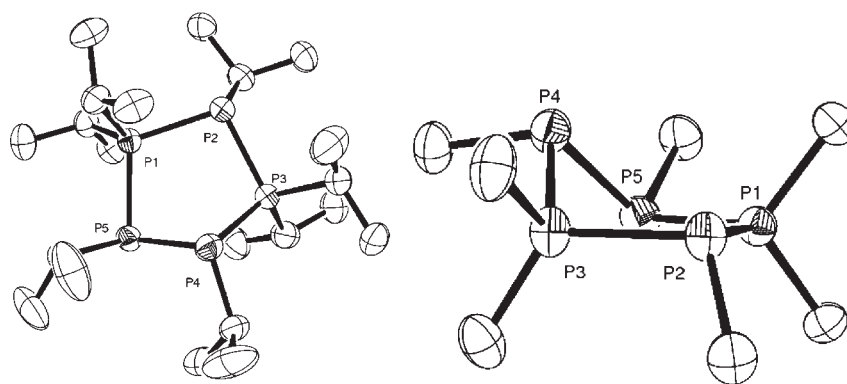


**Figure 3.** ORTEP views of the cation in  $[11(^i\text{Pr})][\text{GaCl}_4]_2 \cdot \text{CH}_2\text{Cl}_2$ . Thermal ellipsoids are shown at the 50% probability level. Carbon atoms are unlabeled, and hydrogen atoms are omitted for clarity. The right view shows only the phosphorus framework and associated  $\alpha$  carbons, indicating an  ${}^4E$  conformation.

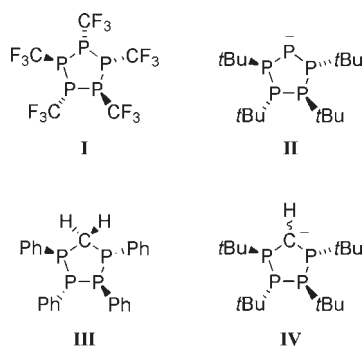
**Table 3.** Selected Homoatomic Distances ( $\text{\AA}$ ) and Bond Angles ( $\text{deg}$ )<sup>a</sup> in the Solid State Structure of  $[11(^i\text{Pr})][\text{GaCl}_4]_2 \cdot \text{CH}_2\text{Cl}_2$  and Comparative Values for  $11'$  and  $11''$ <sup>19,b</sup>

	$[11(^i\text{Pr})][\text{GaCl}_4]_2 \cdot \text{CH}_2\text{Cl}_2$	$11'[\text{OTf}]_2$	$11''[\text{OTf}]_2$
P-P Range	2.2022(9)–2.2341(10)	2.199–2.238	2.193(2)–2.234(2)
P-P Average	2.214	2.228	2.213
<b>P-P1-P</b>	<b>109.07(4)</b>	<b>107.17(9)</b>	<b>109.58(8)</b>
P-P2-P	98.43(4)	95.84(10)	95.05(8)
<b>P-P3-P</b>	<b>101.24(4)</b>	<b>109.25(10)</b>	<b>106.26(8)</b>
P-P4-P	94.63(4)	93.99(10)	105.23(7)
P-P5-P	95.56(4)	93.96(9)	101.79(7)
C-P4-P5-C	92.99(14)	100.74(35)	143.23(26)
$\Phi^b$	286.80(5)	312.08(12)	218.14(12)
$Q^b$	0.9040(7)	0.8922(19)	0.6614(14)
Pseudorotational Conformation	${}^4E$	${}^4T_5$	${}^2E$

<sup>a</sup> Angles indicated in bold center on the phosphonium centers (P1, P3).

<sup>b</sup> Also indicated are the calculated Cremer–Pople<sup>25,26</sup> puckering angle ( $\Phi$ , deg), puckering parameter ( $Q$ ,  $\text{\AA}$ ), and conformation.

solution for  $11(^i\text{Pr})$ , it is instructive to compare it directly with the analogous monocation **10**.



For monocations **10**, pseudorotation provides sufficient rationale for the observation ( ${}^{31}\text{P}\{^1\text{H}\}$  NMR) of effective  $C_2$  symmetry in derivatives with symmetric substituents at the

phosphonium center and effective  $C_1$  symmetry in asymmetrically substituted derivatives. Pseudorotation is, however, insufficient to explain the symmetry observed in high temperature NMR spectra of  $11(^i\text{Pr})$ , as even a time-averaged planar structure presents only  $C_1$  symmetry. Inversion at phosphorus may be additionally invoked to rationalize the observed AMM'XX' spin system at high temperatures.

The significant steric strain imposed by the multiple isopropyl substituents in  $11(^i\text{Pr})$  may promote comparatively rapid inversion at P2 or P4/P5, as shown in Scheme 3. Assuming a first-order mechanism, the activation parameters for this process, which effectively exchanges the resonances of P1/P3 and P4/P5, were calculated by line-shape analysis of  ${}^{31}\text{P}\{^1\text{H}\}$  NMR spectra between 246 and 292 K (Figure 6). In EtCN at 298 K, the free energy of activation  $\Delta G^\ddagger$  was determined to be  $52 \pm 1.5 \text{ kJ} \cdot \text{mol}^{-1}$  (95% C.I. by weighted linear regression). This is in good agreement with a barrier of  $50 \text{ kJ} \cdot \text{mol}^{-1}$  estimated<sup>33</sup> using an approximate coalescence temperature ( $T_c$ ) of 277 K. This is significantly lower than the previously determined barrier for the inversion of substituted diphosphines<sup>34</sup> ( $94$ – $100 \text{ kJ} \cdot \text{mol}^{-1}$ ) or phosphorus cages ( $77$ – $126 \text{ kJ} \cdot \text{mol}^{-1}$ ).<sup>6</sup>

However, the mechanism of this inversion process is not unambiguous. In addition to the steric requirements of the  ${}^i\text{Pr}$  substituents, the lower inversion barrier in  $11(^i\text{Pr})$  could alternatively be rationalized by invoking partial double bond character along P1–P2–P3. Furthermore, in light of the solution ring-opening reactions of this species (*vide infra*), an intermolecular reaction of  $11(^i\text{Pr})$  with free chloride ions may also be proposed as a low-energy pathway for net inversion. Previous experimental and computational work from Humbel and co-workers has indicated that an HCl-induced inversion pathway might reduce the inversion barrier for chlorophosphines to  $\sim 40 \text{ kJ} \cdot \text{mol}^{-1}$ .<sup>35</sup> It is possible that a similar interaction occurs between P2 in  $11(^i\text{Pr})$  and a tetrachlorogallate anion. Heated solutions of  $[11(^i\text{Pr})][\text{GaCl}_4]_2$  in EtCN give a single product that is tentatively assigned as  $[8(^i\text{Pr})][\text{GaCl}_4]$  on the basis of the  ${}^{31}\text{P}$  and  ${}^1\text{H}$  NMR parameters (Scheme 4).

As the reductive coupling reactions for derivatives of **4** $[\text{GaCl}_4]$  result in the assembly of alkyl and aryl cyclophosphinophosphonium cations, analogous reactions of the chlorophosphinodichlorophosphonium  $[5(\text{Ph})][\text{GaCl}_4]$  yield a new chloro-substituted cyclophosphinophosphonium  $[10'(\text{Ph})][\text{GaCl}_4]$  (Scheme 5), which is identified using  ${}^{31}\text{P}$  NMR spectroscopy (Figure 7; Table 5).

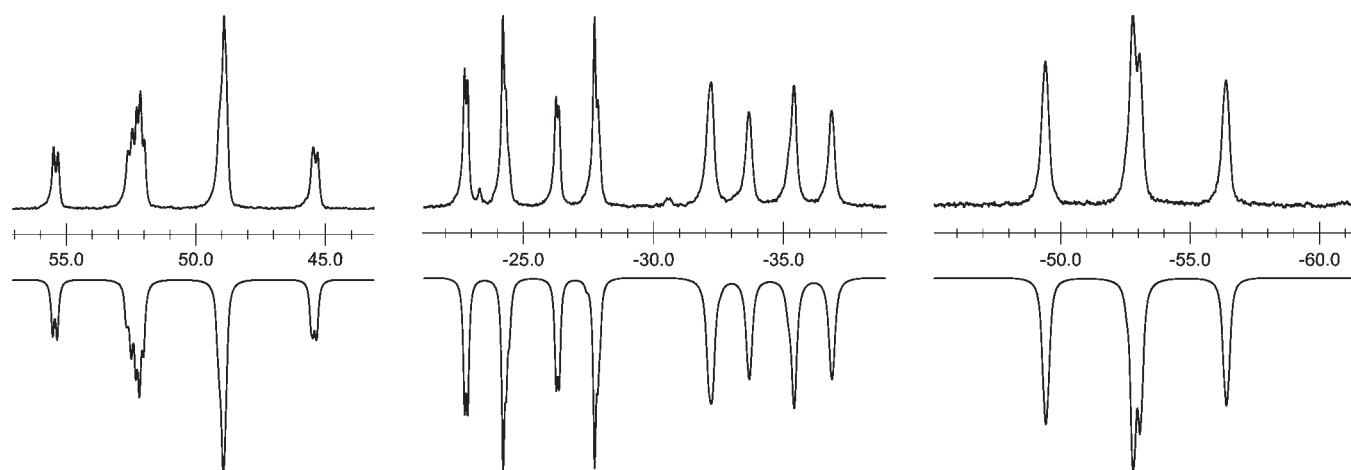


**Figure 4.** Experimental (upright) and simulated (inverted) expansions of the  $^{31}\text{P}\{^1\text{H}\}$  NMR spectrum of  $[\mathbf{11}(\text{iPr})][\text{GaCl}_4]_2$  in EtCN at 101.3 MHz and 188 K. Parameters for the AGHMX spin system are collected in Table 4.

**Table 4.**  $^{31}\text{P}\{^1\text{H}\}$  NMR Parameters<sup>a</sup> for  $[\mathbf{11}(\text{Et})][\text{GaCl}_4]_2$ ,  $[\mathbf{11}(\text{iPr})][\text{GaCl}_4]_2$ , and  $[\mathbf{11}(\text{Ph}_2/\text{Me})][\text{GaCl}_4]_2$  in Comparison with Previously Reported Heteroleptic Derivatives of  $\mathbf{11}[\text{OTf}]^b$

Cation						
		<b>11(Et)</b>	<b>11(iPr)</b>	<b>11(Ph<sub>2</sub>/Me)</b>	<b>11(Me)<sup>19</sup></b>	<b>11<sup>r,19,b</sup></b>
$\delta$ (ppm)	<b>P1</b>	<b>87.3</b>	<b>52.1</b>	<b>72.5</b>	<b>72.6</b>	<b>52.6 [X]</b>
	<b>P2</b>	<b>-30.9</b>	<b>-52.9</b>	<b>-32.5</b>	<b>-20.9</b>	<b>-29.3 [G]</b>
	<b>P3</b>	<b>82.0</b>	<b>48.9</b>	<b>60.7</b>	<b>67.0</b>	<b>42.8 [M]</b>
	<b>P4</b>	<b>-9.6</b>	<b>-25.3</b>	<b>-0.7</b>	<b>-0.2</b>	<b>-23.6 [B]</b>
	<b>P5</b>	<b>-17.0</b>	<b>-34.5</b>	<b>-11.0</b>	<b>-7</b>	<b>-35.4 [A]</b>
$^1J_{\text{PP}}$ (Hz)	<b>P1P2</b>	<b>-332</b>	<b>-340</b>	<b>-320</b>	<b>-314</b>	<b>-327</b>
	<b>P1P5</b>	<b>-354</b>	<b>-326</b>	<b>-349</b>	<b>-327</b>	<b>-379</b>
	<b>P2P3</b>	<b>-317</b>	<b>-367</b>	<b>-307</b>	<b>-302</b>	<b>-338</b>
	<b>P3P4</b>	<b>-345</b>	<b>-360</b>	<b>-339</b>	<b>-320</b>	<b>-335</b>
	<b>P4P5</b>	<b>-306</b>	<b>-149</b>	<b>-260</b>	<b>-274</b>	<b>-313</b>
$^2J_{\text{PP}}$ (Hz)	<b>P1P3</b>	<b>54</b>	<b>-17</b>	<b>36</b>	<b>36</b>	<b>37</b>
	<b>P1P4</b>	<b>6</b>	<b>&lt; 10<sup>c</sup></b>	<b>21</b>	<b>12</b>	<b>1</b>
	<b>P2P4</b>	<b>64</b>	<b>-12</b>	<b>6</b>	<b>5</b>	<b>-13</b>
	<b>P2P5</b>	<b>-18</b>	<b>&lt; 10<sup>c</sup></b>	<b>3</b>	<b>9</b>	<b>-12</b>
	<b>P3P5</b>	<b>21</b>	<b>&lt; 10<sup>c</sup></b>	<b>-14</b>	<b>15</b>	<b>2</b>
Spin system		AGHMX			ABGMX <sup>d</sup>	
T (K)		298	188	298	298	298
Solvent		CH <sub>2</sub> Cl <sub>2</sub>	EtCN	CH <sub>2</sub> Cl <sub>2</sub>	MeCN	MeCN

<sup>a</sup> Bold values indicate parameters involving the phosphonium center(s). All parameters were derived by iterative fitting of experimental data at 101.3 MHz. <sup>b</sup> Substituents at P4 and P5 are *trans*-oriented in all cases. <sup>c</sup> Chemical shift assignments for P1 and P3 were not specified in the original reference. The assignments here are assumed and based on similarities of the magnitude of the chemical shifts but should not be taken as definitive. <sup>d</sup> Line-broadening remains significant at 188 K, so  $|^2J_{\text{PP}}|$  values < 10 Hz could only be approximated. <sup>e</sup> Designation of this spin system according to convention would erroneously imply a first order relationship between P4 and P5. For clarity, an ABGMX designation, as labeled, is used instead.

$^{31}\text{P}\{^1\text{H}\}$  NMR spectra of reaction mixtures of  $\mathbf{5}(\text{Ph})$  with  $\text{SbPh}_3$  initially show the formation of  $\text{PhPCl}_2$  and  $\mathbf{10}'(\text{Ph})$ , followed by the gradual formation of  $\mathbf{10}(\text{Ph})$  (Figure 8), suggesting conversion between  $\mathbf{10}'(\text{Ph})$  and  $\mathbf{10}(\text{Ph})$  by slow Ph/Cl substituent exchange ( $t_{1/2} \cong 6\text{--}7$  days) between phosphorus

and antimony. Substituent exchange behavior, although uncommon for phosphorus, is well-known for antimony<sup>36,37</sup> and appears to be facilitated by  $\text{GaCl}_3$ , as substantiated by the immediate observation ( $^{31}\text{P}$  NMR) of a 1:1 mixture of  $[\mathbf{10}'(\text{Ph})][\text{GaCl}_4]$  and  $[\mathbf{10}(\text{Ph})][\text{GaCl}_4]$  when  $\text{PhPCl}_2$  was

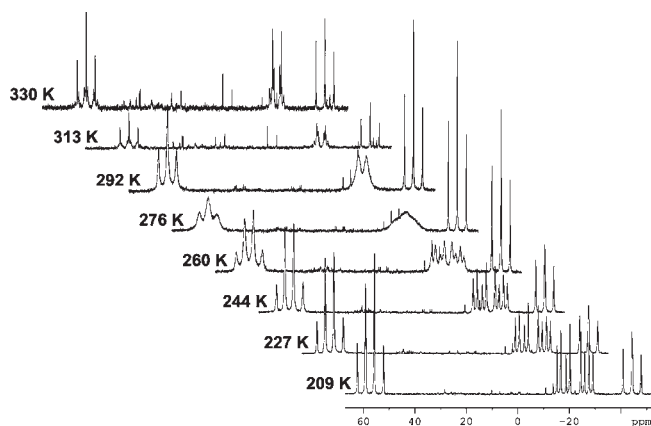


**Figure 5.** Variable-temperature  $^{31}\text{P}\{^1\text{H}\}$  NMR spectra of  $[\mathbf{11}(\text{iPr})][\text{GaCl}_4]_2$  in EtCN at 101.3 MHz.

**Scheme 3. Possible Inversion Pathways for  $\mathbf{11}(\text{iPr})$  Which Effect Time-Averaged  $C_2$  Symmetry**

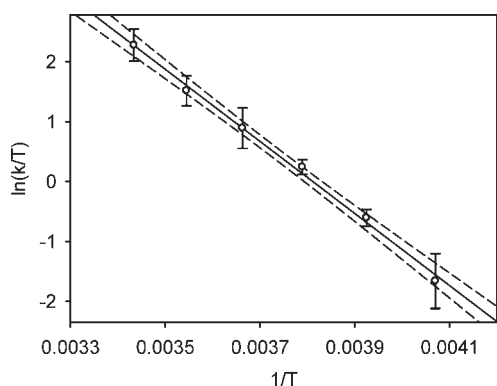
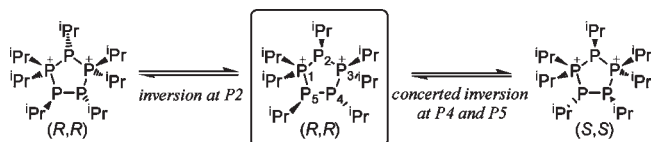
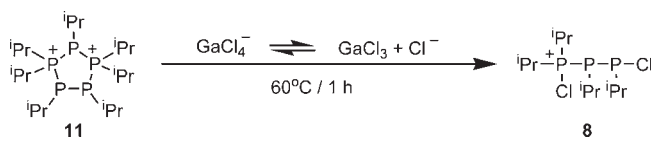


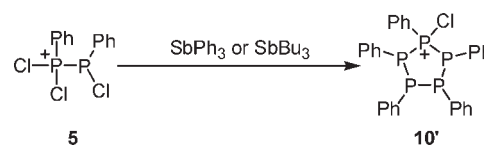
**Figure 6.** Eyring plot for the dynamic behavior of  $[\mathbf{11}(\text{iPr})][\text{GaCl}_4]_2$  in EtCN based on rate constants ( $k$ ) from a line shape analysis of  $^{31}\text{P}\{^1\text{H}\}$  NMR spectra between 246 and 292 K (simulated and experimental spectra available in the Supporting Information). Error bars are plotted on the basis of error estimates in dNMR line shape fitting, and the 95% confidence interval about the regression line is indicated with dashed lines.

**Scheme 4. Ring Opening of  $[\mathbf{11}(\text{iPr})][\text{GaCl}_4]_2$  in EtCN Observed Using  $^{31}\text{P}\{^1\text{H}\}$  NMR Spectroscopy**



added to a 1:1 mixture of  $\text{SbPh}_3/\text{GaCl}_3$ , as well as the generation of  $\mathbf{4}(\text{Ph})$  from  $\mathbf{5}(\text{Ph})$  under the same conditions.

**Scheme 5. Reductive Coupling of  $[\mathbf{5}(\text{Ph})][\text{GaCl}_4]$  to Yield  $[\mathbf{10}'(\text{Ph})][\text{GaCl}_4]$**



**CONCLUSION**

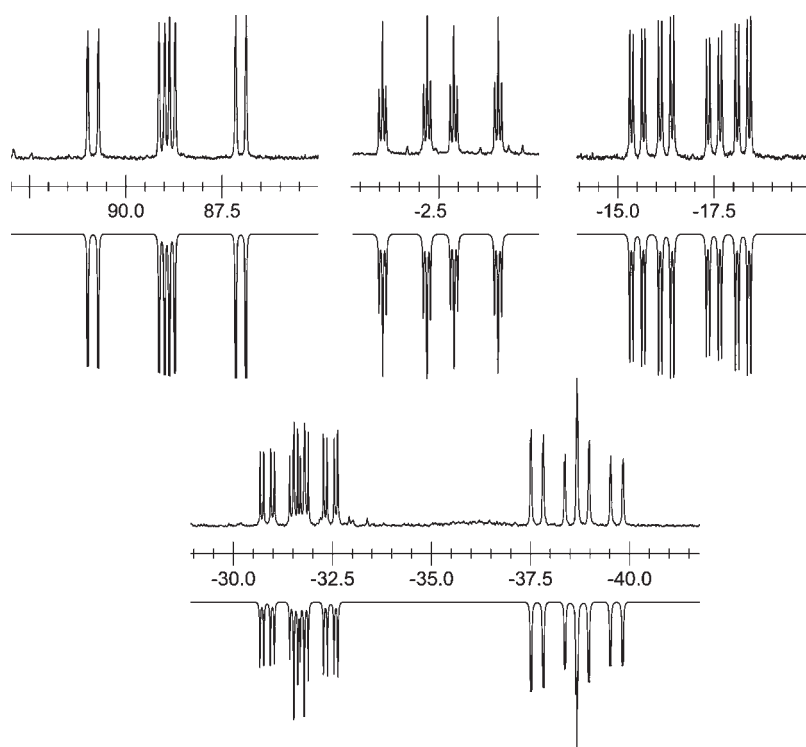
New derivatives of chlorophosphinochlorophosphonium ( $\mathbf{4}$ ) and chlorophosphinodichlorophosphonium ( $\mathbf{5}$ ) cations have been used as synthons for the assembly of larger cationic polyphosphorus frameworks via reductive coupling.  $^{31}\text{P}$  NMR studies of reactions with stibine reducing agents show the dependence of product distribution on stoichiometry and the reductants used. These reactions were shown to readily produce a variety of new and known acyclic and cyclic frameworks, including three new chloro-functionalized cations, highlighted in Chart 3. The first *cis*-substituted derivative of the cyclo-triphosphino-1,3-diphosphonium framework  $[\mathbf{11}(\text{Ph}_2/\text{Me})][\text{GaCl}_4]_2$  has been observed by  $^{31}\text{P}$  NMR spectroscopy, and the solution dynamics have been analyzed in the context of the variable temperature solution spectra and the solid state crystallographic data for  $[\mathbf{11}(\text{iPr})][\text{GaCl}_4]_2$ .

**SYNTHETIC PROCEDURES AND CHARACTERIZATION DATA**

Unless otherwise specified, reactions were carried out in a glovebox under an inert  $\text{N}_2$  atmosphere. Solvents were dried on an MBraun solvent purification system and stored over 4 Å molecular sieves unless otherwise specified. Anhydrous MeCN was purchased from Aldrich, sparged with dry nitrogen or argon, and stored over 3 Å molecular sieves before use, and  $\text{Et}_2\text{O}$  was dried by refluxing it over Na/benzophenone and distilled before use. Deuterated solvents were purchased from Aldrich or Cambridge Isotope Laboratories and stored over molecular sieves for 24 h prior to use.  $\text{Me}_2\text{PCl}$  and  $\text{MePCl}_2$  were purchased from Strem and used as received.  $\text{PPh}_3$ ,  $\text{SbPh}_3$ ,  $\text{CyPCl}_2$ ,  $\text{Et}_2\text{PCl}$ ,  $\text{iPrPCl}_2$ , and  $\text{iPr}_2\text{PCl}$  were purchased from Aldrich and used as received.  $\text{Ph}_2\text{PCl}$ ,  $\text{PhPCl}_2$ ,  $\text{EtPCl}_2$ , and  $\text{Me}_3\text{SiOTf}$  were purchased from Aldrich and purified by vacuum distillation prior to use.  $\text{GaCl}_3$  was purchased from Aldrich or Strem and sublimed under a static vacuum prior to use.  $\text{Sb}^n\text{Bu}_3$  was used as received (supplier unknown).  $[\mathbf{3}(\text{Ph})][\text{GaCl}_4]$  and  $[\mathbf{3}(\text{Me})][\text{GaCl}_4]$  were prepared according to literature methods.<sup>5,16</sup>

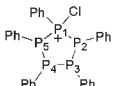
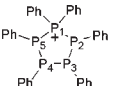
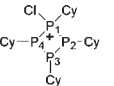
Solution  $^1\text{H}$ ,  $^{13}\text{C}$ , and  $^{31}\text{P}$  NMR spectra were collected at room temperature on Bruker AC-250 (5.9 T) and Bruker Avance 500 (11.7 T) NMR spectrometers. Chemical shifts are reported in parts per million relative to trace protonated solvent ( $^1\text{H}$ ), to perdeuterated solvent ( $^{13}\text{C}$ ), or to an external reference standard ( $^{31}\text{P}$ , 85%  $\text{H}_3\text{PO}_4$ ). NMR spectra of reaction mixtures were obtained by transferring an aliquot of the bulk solution to a 5 mm NMR tube, which was then capped and sealed with Parafilm.  $^{31}\text{P}\{^1\text{H}\}$  NMR integrations are estimated to be accurate to within  $\pm 10\%$  for identical coordination numbers or  $\pm 20\%$  otherwise.<sup>38</sup> All reported  $^{31}\text{P}\{^1\text{H}\}$  NMR parameters for second-order spin systems (except  $[\mathbf{11}(\text{iPr})][\text{GaCl}_4]_2$ ) were derived by iterative simulation of experimental data obtained at both fields ( $^{31}\text{P}$  Larmor frequencies of 101.3 and 202.6 MHz)





**Figure 7.** Experimental (upright) and simulated (inverted) expansions of the  $^{31}\text{P}\{^1\text{H}\}$  NMR spectrum of  $[\mathbf{10}'(\text{Ph})][\text{GaCl}_4]$ , *cyclo*- $[(\text{Ph}_5\text{P}_5)\text{Cl}][\text{GaCl}_4]$ , at 280 K and 202.6 MHz, displaying an AGHMX spin system with a downfield resonance ( $\delta_{\text{X}} = 89$  ppm) characteristic of a Cl-substituted phosphonium center.

**Table 5.**  $^{31}\text{P}\{^1\text{H}\}$  NMR Parameters<sup>a</sup> for  $[\mathbf{10}'(\text{Ph})][\text{GaCl}_4]$  in Comparison to Those for  $[\mathbf{10}(\text{Ph})][\text{OTf}]^{17}$  and  $[\mathbf{9}'(\text{Cy})][\text{OTf}]^{14}$

Cation			
	$\mathbf{10}'(\text{Ph})$	$\mathbf{10}(\text{Ph})^{17}$	$\mathbf{9}'(\text{Cy})^{14}$
$\delta$ (ppm)	<b>89.3</b> [1] -15.7 [2] -30.9 [3] -37.5 [4] -1.2 [5]	<b>22</b> [1] -36 [2/5] -42 [3/4]	<b>95.1</b> [1] -40.7 [2/4] -54.4 [3]
$^1J_{\text{PP}}$ (Hz)	<b>-403</b> [1,2] -374 [1,5] -153 [2,3] -232 [4,5] -174 [3,4]	<b>-325</b> [1,2; 1,5] -142 [2,3; 4,5] -160 [3,4]	<b>-285</b> [1,2; 1,4] -126 [2,3; 3,4]
$^2J_{\text{PP}}$ (Hz)	<b>54</b> [1,3] <b>6</b> [1,4] 64 [2,4] -18 [2,5] 21 [3,5]	<b>28</b> [1,3; 1,4] 79 [2,4; 3,5] -24 [2,5]	18 [1,3]
Spin system	AGHMX	AA'BB'X	AM <sub>2</sub> X
T (K)	298	298	300
Solvent	CH <sub>2</sub> Cl <sub>2</sub>	CHCl <sub>3</sub>	CH <sub>2</sub> Cl <sub>2</sub>

<sup>a</sup> Numbers in square brackets indicate the phosphorus atoms, as labeled above. Bold values indicate parameters involving the phosphonium center. All parameters were derived by iterative fitting of experimental data at 101.3 MHz.

using gNMR, version 4.0 or 5.0.6.0.<sup>39,40</sup> Typically, the higher field experimental spectrum was used to find the spin system parameters, and the lower field data were subsequently used to ensure that the parameters were valid at both fields. For  $[\mathbf{11}(\text{Pr})][\text{GaCl}_4]_2$ , only data acquired at 188 K and 101.3 MHz were used for iterative fitting and determination of  $^{31}\text{P}\{^1\text{H}\}$  NMR parameters. For  $[\mathbf{10}'(\text{Ph})][\text{GaCl}_4]$ , data acquired at 298 K and 202.6 MHz showed line broadening that prevented a viable simulation, so the sample was cooled to 280 K. The signs of the P–P coupling constants reported in Table 4 have been established by assigning the  $^1J_{\text{PP}}$  coupling constants as negative.<sup>24,41</sup> Letter designations for the phosphorus spin systems have been assigned by calculating the ratio  $|\Delta\nu/J|$ , where  $\Delta\nu$  is the difference in  $^{31}\text{P}$  chemical shifts in Hertz, and using a value of 10 at the lower field as the threshold between a first and second order letter designation. Temperatures reported above 298 K for  $^{31}\text{P}\{^1\text{H}\}$  NMR spectra of  $[\mathbf{11}(\text{Pr})][\text{GaCl}_4]_2$  were calibrated against a neat ethylene glycol standard according to equations reported by Ammann et al.<sup>42</sup> Temperatures below 298 K are reported on the basis of a linear plot of observed temperatures vs temperatures calculated<sup>42</sup> from  $^1\text{H}$  NMR measurements of a neat MeOH standard over the range 188–309 K. Rate constants  $k$  for the solution dynamics of  $[\mathbf{11}(\text{Pr})][\text{GaCl}_4]_2$  in EtCN (*ca.* 0.04 M) were calculated by line-shape analysis using dynamic NMR as implemented in gNMR, version 5.0.6.0,<sup>40</sup> assuming a two site exchange between P1/P3 and P4/P5. Simulated and experimental  $^{31}\text{P}\{^1\text{H}\}$  NMR spectra included in this analysis are included in the Supporting Information. Data from temperatures above 292 K were omitted owing to observed thermal decomposition of  $\mathbf{11}(\text{Pr})$  to  $\mathbf{8}(\text{Pr})$ . Data from temperatures below 246 K were omitted, as the small magnitude rate constants resulted in

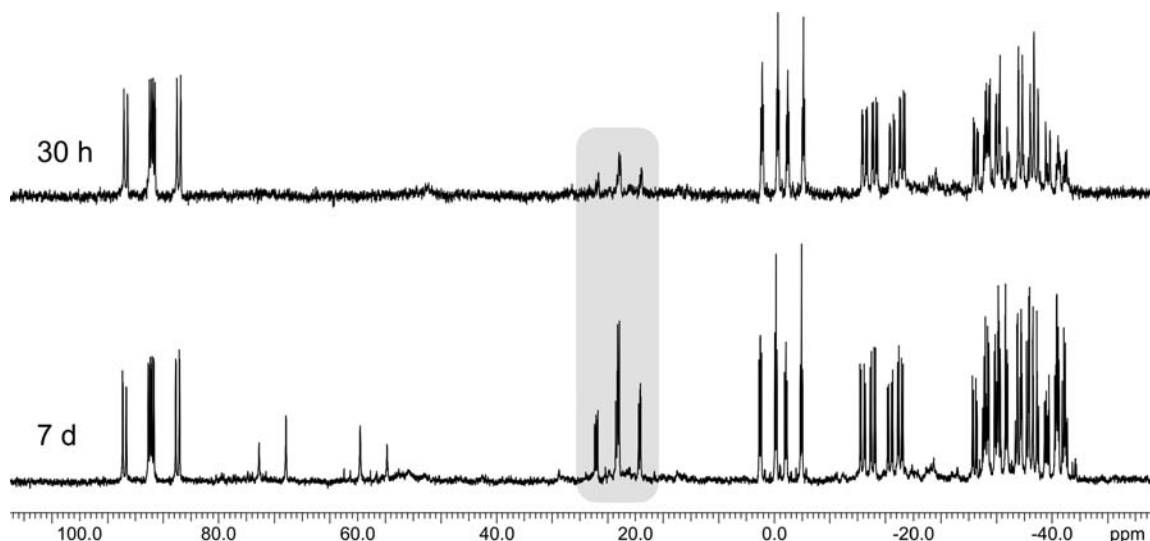
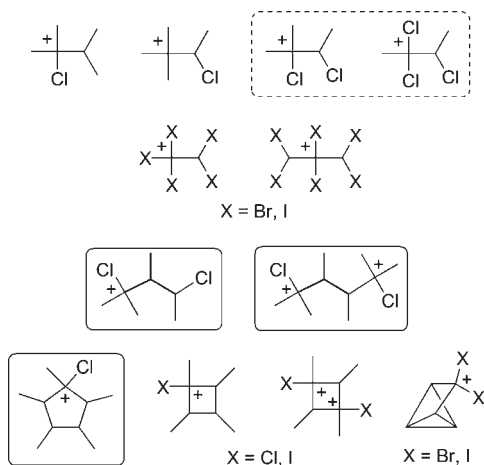


**Figure 8.**  $^{31}\text{P}\{^1\text{H}\}$  NMR spectrum of the reaction mixture of  $[\mathbf{5}(\text{Ph})][\text{GaCl}_4]$  with  $\text{SbPh}_3$  after 30 h (top) and 7 days (bottom) at 101.3 MHz, indicating the transformation of  $[\mathbf{10}'(\text{Ph})][\text{GaCl}_4]$  to  $[\mathbf{10}(\text{Ph})][\text{GaCl}_4]$ .  $t_{1/2}$  was estimated by integration of the well-separated phosphonium resonances in  $[\mathbf{10}(\text{Ph})][\text{GaCl}_4]$  (shaded) vs.  $[\mathbf{10}'(\text{Ph})][\text{GaCl}_4]$ . The remaining  $^{31}\text{P}$  resonances for  $[\mathbf{10}(\text{Ph})][\text{GaCl}_4]$  overlap with those of  $[\mathbf{10}'(\text{Ph})][\text{GaCl}_4]$  in the region between  $-25$  and  $-45$  ppm.  $\text{PhPCl}_2$  (162 ppm, not shown) is also present.

### Chart 3. Framework Drawings of Halide-Functionalized catena-Phosphinophosphonium Cations<sup>a</sup>



<sup>a</sup>Vertices represent phosphorus atoms. The first derivatives of frameworks in boxes are reported here as products of the reductive coupling of the phosphinophosphonium cations in the dotted box.

estimated errors in  $k$  on the same order of magnitude as  $k$  itself. Weighted linear regression and error analysis of the Eyring plot data  $[\ln(k/T)]$  versus  $1/T$ <sup>43</sup> were performed using Octave<sup>44</sup> and plotted using Sigmaplot.<sup>45</sup> Details of the regression and error analysis for  $\Delta H^\ddagger$ ,  $\Delta S^\ddagger$ , and  $\Delta G^\ddagger$  can be found in the Supporting Information.

Single crystal X-ray diffraction data were collected on a Bruker D8/APEX II CCD diffractometer at 173 K using  $\omega$  scans with a width of  $0.3^\circ$  and 15 s exposures. All measurements were made with graphite monochromated Mo  $K\alpha$  radiation (0.71073 Å). The data were corrected for absorption through Gaussian integration from indexing of the crystal faces. The structures were solved by direct methods (SHELXS-97<sup>46</sup>) and refined using full-matrix least-squares on  $F^2$  (SHELXL-97<sup>46</sup>). All non-hydrogen

atoms were refined anisotropically, while hydrogen atoms were assigned positions based on the  $sp^2$  or  $sp^3$  hybridization geometries of their attached carbons and were given thermal parameters 20% greater than those of their parent atoms.

Electrospray ionization mass spectrometric (ESI-MS) analyses were performed on a Bruker Daltonics microTOF instrument in both positive and negative ion modes. Instrument parameters were set as follows: spray voltage, 4500 V (positive) or 3300 V (negative); nebulizer gas ( $\text{N}_2$ ), 1 bar; dry gas ( $\text{N}_2$ ), 4 L/min; dry temperature, 180 °C; exit voltage of the heated capillary, 130 V (positive) or 90 V (negative); and sample flow rate, 2  $\mu\text{L}/\text{min}$ . Observed peaks with intensities  $\geq 2\%$  relative to the base peak are reported.

The melting point of  $[\mathbf{11}(\text{Pr})][\text{GaCl}_4]_2$  was obtained using an electrothermal apparatus on crushed crystalline material flame-sealed in a glass capillary under dry nitrogen. Infrared spectra of the crystals of  $[\mathbf{11}(\text{Pr})][\text{GaCl}_4]_2$  were obtained as a Nujol mull, so C–H stretching frequencies were obscured.

**Sample Preparation for Derivatives of  $[\text{R}_2(\text{Cl})\text{P}-\text{PR}'\text{Cl}][\text{GaCl}_4]$ ,  $4[\text{GaCl}_4]$ .** The addition of  $\text{R}'\text{PCl}_2$  (0.20 mmol) and then  $\text{R}_2\text{PCl}$  (0.20 mmol) to a stirring solution of  $\text{GaCl}_3$  (35 mg, 0.20 mmol) in  $\text{CH}_2\text{Cl}_2$  (1 mL) afforded a pale yellow solution, which showed virtually quantitative formation of  $4[\text{GaCl}_4]$  (>99% by  $^{31}\text{P}$  NMR) after 1 h at room temperature. Solvent removal *in vacuo* or the addition of  $\text{Et}_2\text{O}$  or pentane yielded an oil.

**Sample Preparation for Derivatives of  $[\text{R}(\text{Cl})_2\text{P}-\text{PRCl}][\text{GaCl}_4]$ ,  $5[\text{GaCl}_4]$ .**  $\text{RPCl}_2$  (0.40 mmol) was added to a stirring solution of  $\text{GaCl}_3$  (35 mg, 0.20 mmol) in  $\text{CH}_2\text{Cl}_2$  (1 mL). The formation of  $5[\text{GaCl}_4]$  was quantitative (>99% by  $^{31}\text{P}$  NMR) after 30–60 min at room temperature. Removal of the solvent *in vacuo* or the addition of  $\text{Et}_2\text{O}$  or pentane yielded an oil.

**Generalized Procedure for Reductive Coupling Reactions.** Phosphinophosphonium salts  $3-5[\text{GaCl}_4]$  (0.2–0.3 mmol) were synthesized *in situ* and allowed to stir for 30 min to 1 h in 0.7–1 mL of  $\text{CH}_2\text{Cl}_2$  (unless otherwise noted) before the

addition of either tri-*n*-butylstibine or triphenylstibine. For reactions involving 1 equivalent of SbPh<sub>3</sub> or less, phosphinophosphonium salts were initially synthesized in 0.5 mL of CH<sub>2</sub>Cl<sub>2</sub>, and SbPh<sub>3</sub> was dissolved in another 0.5 mL of CH<sub>2</sub>Cl<sub>2</sub> to be added by pipet. Otherwise, the solution of phosphinophosphonium gallate was transferred directly onto solid SbPh<sub>3</sub> by pipet. SbBu<sub>3</sub> was added directly to the stirring solution by micropipet. For reactions involving additional equivalent(s) of GaCl<sub>3</sub>, these were weighed out and added to the initial solution of the phosphinophosphonium gallate, before the addition of any reducing agent. Solutions were allowed to stir at room temperature for 1 h and 18–24 h before NMR spectra were collected. Reactions of **4**(Me) resulted in the precipitation of CH<sub>2</sub>Cl<sub>2</sub>-insoluble solids, so reaction mixtures were filtered through a pipet filter. The isolated solids were washed with CH<sub>2</sub>Cl<sub>2</sub> and dissolved in MeCN, so that both the supernatant and precipitate could be analyzed separately by <sup>31</sup>P NMR spectroscopy.

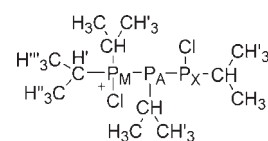
**NMR Observation of [Et<sub>2</sub>(Cl)P<sub>X</sub>-P<sub>A</sub>Et-P<sub>A</sub>Et-P<sub>X</sub>(Cl)Et<sub>2</sub>][GaCl<sub>4</sub>]<sub>2</sub>, [7'(Et)][GaCl<sub>4</sub>]<sub>2</sub> and cyclo-[Et<sub>7</sub>P<sub>5</sub>][GaCl<sub>4</sub>]<sub>2</sub>, [11(Et)][GaCl<sub>4</sub>]<sub>2</sub>.** Following the generalized procedure for reductive coupling, [4(Et)][GaCl<sub>4</sub>] was synthesized *in situ* (0.3 mmol) and reacted in a ratio of 1:1:2 equivalents of 4(Et)/GaCl<sub>3</sub>/SbPh<sub>3</sub>. <sup>31</sup>P{<sup>1</sup>H} NMR spectra (101.3 MHz, 298 K, CH<sub>2</sub>Cl<sub>2</sub>) collected after 1 h indicated nearly quantitative conversion to a single product with an AA'BB' spin system, assigned as 7'(Et) [ $\delta_A = 111$ ,  $\delta_X = -38$ ,  $^1J_{AA'} = -271$  Hz,  $^1J_{AX} = ^1J_{AX'} = -374$  Hz,  $^2J_{AX'} = ^2J_{AX} = 86$  Hz,  $^3J_{XX'} = 84$  Hz]. Attempted crystallization by vapor diffusion of pentane into the reaction mixture yielded a viscous oil, which, upon standing for 6 months, gave rise to a colorless semicrystalline material coated in yellow oil. <sup>31</sup>P{<sup>1</sup>H} NMR spectra of the inseparable redissolved material showed effectively complete conversion to [11(Et)][GaCl<sub>4</sub>]<sub>2</sub>. <sup>1</sup>H NMR spectra indicated that the mixture was predominantly composed of [11(Et)][GaCl<sub>4</sub>]<sub>2</sub> and the oxidized antimony byproduct [Ph<sub>3</sub>SbCl][GaCl<sub>4</sub>] or Ph<sub>3</sub>SbCl<sub>2</sub>.

**NMR Observation of cyclo-[(MeP)<sub>3</sub>(PPh<sub>2</sub>)<sub>2</sub>][GaCl<sub>4</sub>]<sub>2</sub>, [11(Ph<sub>2</sub>/Me)][GaCl<sub>4</sub>]<sub>2</sub>.** Following the generalized procedure for reductive coupling, [4(Ph<sub>2</sub>/Me)][GaCl<sub>4</sub>] was synthesized *in situ* (0.3 mmol) and reacted with 0, 1, or 2 equivalents of GaCl<sub>3</sub> and either 1 equivalent of SbBu<sub>3</sub> or 1–2 equivalents of SbPh<sub>3</sub>. <sup>31</sup>P{<sup>1</sup>H} NMR spectra collected after 18 h indicated **11**(Ph<sub>2</sub>/Me) and 3(Ph) as the major products, along with 3–20% of 13(Ph<sub>2</sub>/Me). In all cases, the ratio of the *trans/cis* isomers of **11** was approximately 2:1, as assessed by the relative areas of the <sup>31</sup>P{<sup>1</sup>H} NMR resonances. <sup>31</sup>P{<sup>1</sup>H} NMR of [11(Ph<sub>2</sub>/Me)][GaCl<sub>4</sub>]<sub>2</sub> (101.3 MHz, 298 K, CH<sub>2</sub>Cl<sub>2</sub>): *trans*-isomer—AGHMX spin system, see Table 4; *cis*-isomer—ABB'XX' spin system:  $\delta_A = -63.3$ ,  $\delta_B = -34.4$ ,  $\delta_X = 52.8$ ,  $^1J_{AX} = ^1J_{AX'} = -314$  Hz,  $^1J_{BX} = ^1J_{BX'} = -350$  Hz,  $^1J_{BB'} = -323$  Hz,  $^2J_{BX'} = ^2J_{BX} = 17$  Hz,  $^2J_{AB} = 10$  Hz,  $^2J_{AB'} = 2$  Hz,  $^2J_{XX'} = 21$  Hz.

**Synthesis of cyclo-[<sup>i</sup>Pr<sub>7</sub>P<sub>5</sub>][GaCl<sub>4</sub>]<sub>2</sub>, [11(<sup>i</sup>Pr)][GaCl<sub>4</sub>]<sub>2</sub>.** [<sup>i</sup>Pr<sub>2</sub>(Cl)P-P<sup>i</sup>PrCl][GaCl<sub>4</sub>], [4(<sup>i</sup>Pr)][GaCl<sub>4</sub>] (0.3 mmol), was synthesized *in situ* in 0.7 mL of CH<sub>2</sub>Cl<sub>2</sub> according to the generalized procedure (*vide supra*) and allowed to stir for 1 h at room temperature prior to the addition of SbBu<sub>3</sub> (73.8  $\mu$ L, 0.3 mmol). No readily identifiable products could be distinguished from the reaction solution by <sup>31</sup>P{<sup>1</sup>H} NMR spectroscopy after 1.5 h. Upon standing for 20–24 h in an NMR sample tube, colorless crystals suitable for X-ray diffraction precipitated from the reaction solution. The solution was decanted, and the crystals were washed with 2  $\times$  1 mL CH<sub>2</sub>Cl<sub>2</sub> and dried. Yield: 26 mg (0.030 mmol, 30%). D.p. 178–182 °C. An elemental analysis

was not performed owing to the observed decomposition at elevated temperatures. Low temperature resolution of <sup>1</sup>H/<sup>13</sup>C NMR peaks could not be achieved. FT-IR (nujol mull, cm<sup>-1</sup>, [intensity]): 1275 [m], 1222 [s], 1024 [s], 935 [w], 901 [m], 884 [m], 739 [w], 705 [m], 538 [m], 419 [s]. ESI-MS (10<sup>-5</sup> M in MeCN), positive ion mode [ $m/z$  (relative intensity, assignment)]: -223.1 (4, [<sup>i</sup>Pr<sub>3</sub>P<sub>3</sub> + H]<sup>+</sup>), 242.3 (3, unassigned), 265.1 (100, [<sup>i</sup>Pr<sub>4</sub>P<sub>3</sub>]<sup>+</sup>), 299.1 (4, unassigned), 306.2 (6, [<sup>i</sup>Pr<sub>4</sub>P<sub>3</sub> + MeCN]<sup>+</sup>), 339.2 (51, [<sup>i</sup>Pr<sub>5</sub>P<sub>4</sub>]<sup>+</sup>), 413.3 (7, [<sup>i</sup>Pr<sub>6</sub>P<sub>5</sub>]<sup>+</sup>), 429.2 (6, [<sup>i</sup>Pr<sub>4</sub>P<sub>3</sub> + 4MeCN]<sup>+</sup>), 445.1 (3, unassigned); negative ion mode, [GaCl<sub>4</sub>]<sup>-</sup> confirmed by isotope pattern analysis (base peak: 210.8). Crystal data: C<sub>21</sub>H<sub>49</sub>Cl<sub>8</sub>Ga<sub>2</sub>P<sub>5</sub> · CH<sub>2</sub>Cl<sub>2</sub>, fw 964.42; colorless blocks, crystal size 0.58  $\times$  0.41  $\times$  0.34 mm; monoclinic,  $P2_1/n$ ,  $a = 11.6226(11)$  Å,  $b = 22.014(2)$  Å,  $c = 16.9005(15)$  Å,  $\beta = 98.2769(11)^\circ$ ,  $V = 4279.0(7)$  Å<sup>3</sup>,  $Z = 2$ ,  $\mu = 2.086$  mm<sup>-1</sup>;  $2\theta_{\max} = 54.92^\circ$ , collected (independent) reflections = 37146 (9779); 380 refined parameters,  $R_1 (I > 2\sigma(I)) = 0.0399$ ,  $wR_2$  (all data) = 0.1136, GOF = 1.025,  $\Delta\rho_{\max/\min} = 1.041/-0.777$  eÅ<sup>-3</sup>.

**Proposed synthesis of [<sup>i</sup>Pr<sub>2</sub>(Cl)P-P<sup>i</sup>Pr-P<sup>i</sup>PrCl][Ga<sub>x</sub>Cl<sub>y</sub>]<sub>z</sub>, [8(<sup>i</sup>Pr)][Ga<sub>x</sub>Cl<sub>y</sub>]<sub>z</sub>**



A sample of [11(<sup>i</sup>Pr)][GaCl<sub>4</sub>]<sub>2</sub> (26 mg, 0.029 mmol) in EtCN was heated in an NMR tube at 60 °C for 1 h under Ar, after which time, complete conversion to 8(<sup>i</sup>Pr) was indicated by <sup>31</sup>P{<sup>1</sup>H} spectroscopy. Removal of the solvent *in vacuo* yielded an oil. Yield: 18.4 mg (0.034 mmol, based on a GaCl<sub>4</sub> anion). <sup>31</sup>P{<sup>1</sup>H} NMR (EtCN, 101.3 MHz, 294 K): AMX spin system  $\delta_A = -79$ ,  $\delta_M(\text{phosphonium}) = 96$ ,  $\delta_X = 132$ ;  $^1J_{AM} = -375$  Hz,  $^1J_{AM} = -224$  Hz,  $^2J_{MX} = 29$  Hz. <sup>1</sup>H{<sup>31</sup>P} NMR (CD<sub>2</sub>Cl<sub>2</sub>, 500.1 MHz, 298K):  $\delta = 1.22$  (broad s, 3H, -P<sub>A</sub>CHCH<sub>3</sub>), 1.27 (d, 3H, -P<sub>X</sub>CHCH<sub>3</sub>), 1.31 (d, -P<sub>A</sub>CHCH<sub>3</sub>) and 1.33 (broad s, -P<sub>M</sub>CH<sup>7</sup>CH<sup>3</sup>) [6H together], 1.37 (broad s, 3H, -P<sub>M</sub>CHCH<sub>3</sub>), 1.42 (broad s, 3H, -P<sub>M</sub>CHCH<sub>3</sub>), 1.48 (d, 3H, -P<sub>X</sub>CHCH<sub>3</sub>), 1.63 (d, 3H, -P<sub>M</sub>CH<sup>7</sup>CH<sup>3</sup>), 2.45 (sept, 1H, -P<sub>A</sub>CH), 2.63 (sept, 1H, -P<sub>M</sub>CH), 2.95 (sept, 1H, -P<sub>M</sub>CH), 3.17 ppm (sept, 2H, -P<sub>X</sub>CH). Assignment of <sup>1</sup>H resonances was based on <sup>1</sup>H-<sup>1</sup>H COSY NMR, chemical shift, and observed <sup>1</sup>H-<sup>31</sup>P coupling in <sup>1</sup>H NMR spectra. <sup>13</sup>C NMR (d<sub>3</sub>-MeCN, 125.8 MHz, 298K): 17.6–18.96 (overlapping signals in HSQC, -CH<sub>3</sub>), 21.4 (m, -P<sub>M</sub>CH), 23.2 (m, -P<sub>X</sub>CH), 24.0 (m, -P<sub>M</sub>CH), 31.2 (m, -P<sub>A</sub>CH). Assignment of <sup>1</sup>H resonances was based on <sup>13</sup>C-<sup>1</sup>H HSQC NMR spectra. ESI-MS (10<sup>-5</sup> M in MeCN), positive ion mode [ $m/z$  (relative intensity, assignment)]: -223.2 (4, [<sup>i</sup>Pr<sub>3</sub>P<sub>3</sub> + H]<sup>+</sup>), 265.1 (100, [<sup>i</sup>Pr<sub>4</sub>P<sub>3</sub>]<sup>+</sup>), 320.2 (3, [<sup>i</sup>Pr<sub>4</sub>P<sub>3</sub> + EtCN]<sup>+</sup>), 339.2 (2, [<sup>i</sup>Pr<sub>5</sub>P<sub>4</sub>]<sup>+</sup>); negative ion mode, [GaCl<sub>4</sub>]<sup>-</sup> confirmed by isotope pattern analysis (base peak: 210.8).

## ■ ASSOCIATED CONTENT

**S Supporting Information.** Comparisons of simulated and experimental <sup>31</sup>P{<sup>1</sup>H} NMR spectra for line shape analysis, calculated rate constants, numerical values for the reductive coupling product ratios in Table 2, and the crystallographic information file (CIF) for [11(<sup>i</sup>Pr)][GaCl<sub>4</sub>]<sub>2</sub>. This material is available free of charge via the Internet at <http://pubs.acs.org>.

## AUTHOR INFORMATION

## Corresponding Author

\*E-mail: Neil.Burford@dal.ca.

## ACKNOWLEDGMENT

We thank the Natural Sciences and Engineering Research Council of Canada, the Killam Foundation, the Canada Research Chairs Program, the Canada Foundation for Innovation, the Nova Scotia Research and Innovation Trust Fund, the Walter C. Sumner Foundation, and the Eliza Ritchie Scholarship for funding, as well as Prof. Peter D. Wentzell for assistance and advice on error analysis in linear regression.

## REFERENCES

- (1) Dyker, C. A.; Burford, N. *Chem. Asian J.* **2008**, *3*, 28–36.
- (2) Dyker, C. A.; Burford, N.; Lumsden, M. D.; Decken, A. J. *Am. Chem. Soc.* **2006**, *128*, 9632–9633.
- (3) Carpenter, Y.; Dyker, C. A.; Burford, N.; Lumsden, M. D.; Decken, A. J. *Am. Chem. Soc.* **2008**, *130*, 15732–15741.
- (4) Burford, N.; Cameron, T. S.; Ragogna, P. J.; Ocampo-Mavarez, E.; Gee, M.; McDonald, R.; Wasylshen, R. E. *J. Am. Chem. Soc.* **2001**, *123*, 7947–7948.
- (5) Burford, N.; Ragogna, P. J.; McDonald, R.; Ferguson, M. J. *Am. Chem. Soc.* **2003**, *125*, 14404–14410.
- (6) Baudler, M.; Glinka, K. *Chem. Rev.* **1993**, *93*, 1623–1667 and references therein.
- (7) Tarasova, R. I.; Zykova, T. V.; Shagvaleev, F. Sh.; Sitdikova, T. Sh.; Moskva, V. V. *Zh. Obshch. Khim.* **1989**, *60*, 1775–1779.
- (8) Tarasova, R. I.; Sitdikova, T. Sh.; Zykova, T. V.; Shagvaleev, F. Sh.; Moskva, V. V.; Kormachev, V. V.; Rusanov, V. M.; Baranov, Yu. I.; Danilov, S. D. . U.S.S.R. Patent SU 1449565, July 1, 1989; Scifinder Scholar: 1989:497499.
- (9) Shagvaleev, F. Sh.; Zykova, T. V.; Tarasova, R. I.; Sitdikova, T. Sh.; Moskva, V. V. *Zh. Obshch. Khim.* **1990**, *60*, 1775–1779.
- (10) Tarasova, R. I.; Zykova, T. V.; Shagvaleev, F. Sh.; Sitdikova, T. Sh.; Moskva, V. V. *Zh. Obshch. Khim.* **1991**, *61*, 2529–2532.
- (11) Krossing, I.; Raabe, I. *Angew. Chem., Int. Ed. Engl.* **2001**, *40*, 4406–4409.
- (12) Gonsior, M.; Krossing, I.; Müller, L.; Raabe, I.; Jansen, M.; van Wüllen, L. *Chem.—Eur. J.* **2002**, *8*, 4475–4492.
- (13) Krossing, I. *Dalton Trans.* **2002**, 500–512.
- (14) Weigand, J. J.; Burford, N.; Davidson, R. J.; Cameron, T. S.; Seelheim, P. J. *Am. Chem. Soc.* **2009**, *131*, 17943–17953.
- (15) Schmidpeter, A.; Lochschmidt, S.; Sheldrick, W. S. *Angew. Chem., Int. Ed.* **1985**, *24*, 226–227.
- (16) Burford, N.; Cameron, T. S.; LeBlanc, D. J.; Losier, P.; Sereda, S.; Wu, G. *Organometallics* **1997**, *16*, 4712–4717.
- (17) Dyker, C. A.; Riegel, S. D.; Burford, N.; Lumsden, M. D.; Decken, A. J. *Am. Chem. Soc.* **2007**, *129*, 7464–7474.
- (18) Weigand, J. J.; Burford, N.; Lumsden, M. D.; Decken, A. *Angew. Chem., Int. Ed.* **2006**, *45*, 6733–6737.
- (19) Riegel, S. D.; Burford, N.; Lumsden, M. D.; Decken, A. *Chem. Commun.* **2007**, 4668–4670.
- (20) Albrand, J. P.; Gagnaire, D.; Robert, J. B. *J. Am. Chem. Soc.* **1973**, *95*, 6498–6500.
- (21) Albrand, J. P.; Gagnaire, D.; Robert, J. B. *J. Am. Chem. Soc.* **1974**, *96*, 1643.
- (22) Albrand, J. P.; Robert, J. B. *Chem. Commun.* **1974**, 644–645.
- (23) Albrand, J. P.; Faucher, H.; Gagnaire, D.; Robert, J. B. *Chem. Phys. Lett.* **1976**, *38*, 521–523.
- (24) Forgeron, M. A. M.; Gee, M.; Wasylshen, R. E. *J. Phys. Chem.* **2004**, *108*, 4895–4908.
- (25) Spek, A. L. *J. Appl. Crystallogr.* **2003**, *36*, 7–13.
- (26) Cremer, D.; Pople, J. A. *J. Am. Chem. Soc.* **1975**, *97*, 1354–1358.
- (27) Spencer, C. J.; Simpson, P. G.; Lipscomb, W. N. *Acta Crystallogr.* **1962**, *15*, 509.
- (28) Spencer, C. J.; Lipscomb, W. N. *Acta Crystallogr.* **1961**, *14*, 250–256.
- (29) Schisler, A.; Lonneck, P.; Huniar, U.; Ahlrichs, R.; Hey-Hawkins, E. *Angew. Chem., Int. Ed.* **2001**, *40*, 4217–4219.
- (30) Lex, J.; Baudler, M. Z. *Anorg. Allg. Chem.* **1977**, *431*, 49–60.
- (31) Wolf, R.; Hey-Hawkins, E. *Chem. Commun.* **2004**, 2626–2627.
- (32) Hoffman, P. R.; Caulton, K. G. *Inorg. Chem.* **1975**, *14*, 1997–1999.
- (33) Günther, H. . In *NMR Spectroscopy: Basic Principles Concepts, and Applications in Chemistry*; Wiley: Chichester, U.K., 1992; pp 335–390.
- (34) Lambert, J. B.; Jackson, G. F., III; Mueller, D. C. *J. Am. Chem. Soc.* **1970**, *92*, 3093–3097.
- (35) Humbel, S.; Bertrand, C.; Darcel, C.; Bauduin, C.; Jugé, S. *Inorg. Chem.* **2003**, *42*, 420–427.
- (36) Nunn, M.; Sowerby, D. B.; Wesolek, D. M. *J. Organomet. Chem.* **1983**, *251*, C45–C46.
- (37) Balázs, L.; Breunig, H. J. *Coord. Chem. Rev.* **2004**, *248*, 603–621.
- (38) Huynh, K.; Rivard, E.; LeBlanc, W.; Blackstone, V.; Lough, A. J.; Manners, I. *Inorg. Chem.* **2006**, *45*, 7922–7928.
- (39) Budzelaar, P. H. M. *gNMR for Windows*, 4.0; Cherwell Scientific Publishing Limited: Oxford, U.K., 1997.
- (40) Budzelaar, P. H. M. *gNMR for Windows*, 5.0.6.0; Ivorysoft: Winnipeg, MB, Canada, 2006.
- (41) Finer, E. G.; Harris, R. K. *Prog. Nucl. Magn. Reson. Spectrosc.* **1971**, *6*, 61–118.
- (42) Ammann, C.; Meier, P.; Merbach, A. E. *J. Magn. Reson.* **1982**, *46*, 319–321.
- (43) Sandström, J. *Dynamic NMR Spectroscopy*; Academic Press: London, 1982.
- (44) Eaton, J. W. *Octave*, 3.2.4; University of Wisconsin: Madison, WI, 2010.
- (45) *Sigmaplot for Windows*, 10.0.0.54; Systat Software Inc.: Point Richmond, CA, 2006.
- (46) Sheldrick, G. M. *Acta Crystallogr.* **2008**, *A64*, 112–122.